α-Bungarotoxin Receptors Contain α7 Subunits in Two Different Disulfide-bonded Conformations

Sergey Rakhilin, Renaldo C. Drisdel, Daphna Sagher, Daniel S. McGehee,* Yolanda Vallejo, and William N. Green

Department of Pharmacological and Physiological Sciences, *Department of Anesthesia and Critical Care, University of Chicago, Chicago, Illinois 60637

Abstract. Neuronal nicotinic α7 subunits assemble into cell-surface complexes that neither function nor bind α-bungarotoxin when expressed in tsA201 cells. Functional α-bungarotoxin receptors are expressed if the membrane-spanning and cytoplasmic domains of the α7 subunit are replaced by the homologous regions of the serotonin-3 receptor subunit. Bgt-binding surface receptors assembled from chimeric α7/serotonin-3 subunits contain subunits in two different conformations as shown by differences in redox state and other features of the subunits. In contrast, α7 subunit complexes in the same cell line contain subunits in a single conformation. The appearance of a second α7/serotonin-3 subunit conformation coincides with the formation of α-bungarotoxin–binding sites and intrasubunit disulfide bonding, apparently within the α7 domain of the α7/serotonin-3 chimera. In cell lines of neuronal origin that produce functional α7 receptors, α7 subunits undergo a conformational change similar to α7/serotonin-3 subunits. α7 subunits, thus, can fold and assemble by two different pathways. Subunits in a single conformation assemble into nonfunctional receptors, or subunits expressed in specialized cells undergo additional processing to produce functional, α-bungarotoxin–binding receptors with two α7 conformations. Our results suggest that α7 subunit diversity can be achieved postranslationally and is required for functional homomeric receptors.

Key words: α-bungarotoxin • α7 subunits • nicotinic receptors • protein folding • disulfide bonds

IONOTROPIC neurotransmitter receptors rapidly transduce the chemical signal of the neurotransmitter into an electrical signal at the synapse. Recent studies have established the primary structure of the receptor subunits and provided detailed information about the structure, electrophysiology, and pharmacology of these membrane proteins. In contrast to the ubiquitous studies of receptor structure-function, there have been surprisingly few investigations into the processing, folding, and assembly of newly synthesized receptor subunits. These events appear to be rate-limiting during neurotransmitter receptor biogenesis (Green and Millar, 1995), and are likely to play an important role in controlling synaptic efficacy by regulating the number of functional receptors at synapses.

In this study, we investigated the processing of a neuronal nicotinic acetylcholine receptor (AChR)[1] subunit. AChRs are a class of neurotransmitter receptors comprised of five subunits that surround a central aqueous pore. All AChR subunits share a common membrane topology and significant sequence homology (Unwin, 1993; Karlin and Akabas, 1995; Lindstrom, 1995). These same structural features are common to a family of neurotransmitter-gated ion channels that includes cationic channels, acetylcholine (ACh) and serotonin-3 or 5-hydroxytryptamine-3 ($5HT_3$) receptors, and anionic channels, γ-aminobutyric acid-A ($GABA_A$), and glycine receptors. The best characterized members of this family are the muscle-type AChRs, which consist of a homogenous population of receptors at the neuromuscular junction. In the nervous system, there is considerable diversity in the properties of AChRs, which is due in part to the array of subunit types expressed by neurons. There are eight different ligand-binding subunits (α2–α9) and three structural subunits (β2–β4) that are found primarily in the nervous system

Sergey Rakhilin's present address is Laboratory of Molecular and Cellular Neuroscience, The Rockefeller University, New York, NY 10021.

Address correspondence to William N. Green, Department of Pharmacological and Physiological Sciences, University of Chicago, 947 East 58th Street, Chicago, IL 60637. Tel.: (773) 702-1763. Fax: (773) 702-3774. E-mail: wgreen@midway.uchicago.edu

1. *Abbreviations used in this paper:* 5HT, 5-hydroxytryptamine (serotonin); ACh, acetylcholine; AChR, acetylcholine receptor; Bgt, α-bungarotoxin; BgtR, α-bungarotoxin receptor; HA, hemagglutinin; NEM, *N*-ethylmaleimide; TMR-Bgt, α-bungarotoxin tetramethylrhodamine.

(Sargent, 1993; McGehee and Role, 1995; Role and Berg, 1996). These subunit isoforms have distinct, although overlapping, patterns of expression and assemble into receptor subtypes with different pharmacological and functional properties.

In the nervous system, there are large numbers of high-affinity binding sites for the muscle AChR selective antagonist, α-bungarotoxin (Bgt). Early observations that these sites did not correlate directly with high-affinity nicotine binding, combined with a lack of evidence for Bgt-sensitive nicotinic responses in neurons, led to confusion about the function of these binding sites (for review see Clarke, 1992). This apparent contradiction was resolved, in part, by the cloning of α7 subunits and their expression in *Xenopus* oocytes which produced nicotine-gated currents that are potently inhibited by Bgt (Couturier et al., 1990; Schoepfer et al., 1990; Seguela et al., 1993). Recent studies have shown that functional Bgt-binding receptors (BgtRs) are expressed in many parts of the nervous system (Zorumski et al., 1992; Alkondon and Albuquerque, 1993; Zhang et al., 1994), and may be homomeric receptors composed of five α7 subunits (Chen and Patrick, 1997; Rangwala et al., 1997). The BgtR ion channel is highly permeable to Ca^{2+} (Seguela et al., 1993; Castro and Albuquerque, 1995), enabling subsequent activation of Ca^{2+}-dependent events in neurons including the presynaptic enhancement of neurotransmitter release (Vijayaraghavan et al., 1992; McGehee et al., 1995; Alkondon et al., 1996; Gray et al., 1996). Other studies have shown that activation of BgtRs can result in neurite retraction (Chan and Quik, 1993; Pugh and Berg, 1994) and that their expression is upregulated during the formation of thalamocortical projections (Broide et al., 1996), consistent with a developmental role for BgtRs in establishing cortical circuitry. In addition, BgtRs have been linked to a form of schizophrenia (Freedman et al., 1994, 1997; Breese et al., 1997).

Although α7 subunits form functional BgtRs in *Xenopus* oocytes (Couturier et al., 1990; Schoepfer et al., 1990; Seguela et al., 1993), most mammalian cells do not express Bgt-binding sites when transfected with α7 subunits (Cooper and Millar, 1997; Rangwala et al., 1997). It has been assumed that the explanation for this difference was a failure of subunits to be processed and assembled properly. Here, we show that α7 subunits do assemble and are inserted into the plasma membrane, but that these receptors do not function or bind Bgt. A comparison of these α7 receptors with Bgt-binding receptors revealed differences in processing. In cells expressing Bgt-binding α7 receptors, subunits were folded into two different disulfide-bonded conformations and surface receptors contained both conformations. In contrast, α7 subunits were only folded into a single conformation in cells expressing nonfunctional receptors. Our findings suggest that two different α7 subunit conformations in a receptor are required for receptor function.

Materials and Methods

Subunit Constructs

Chick α7 and chick α7/5HT$_3$ subunit cDNAs were gifts from Dr. J.L. Eisele (Pasteur Institute, Paris, France). These cDNAs were subcloned into a pMT3 expression vector (Swick et al., 1992). A cDNA construct was generated in which the chick α7 subunit was truncated just before the first transmembrane domain at amino acid threonine 208 (West et al., 1997; Wells et al., 1998). All subunits were tagged at the COOH terminus with the hemagglutinin (HA) epitope, a stretch of nine amino acids (YPYDVPDYA; Wilson et al., 1984). The nine HA epitope codons (TACCCATACGACGTCCCAGACTACGCT) and a stop codon were inserted after the last codon of the 3′ translated region of the three subunit cDNAs using the extension overlap method (Ho et al., 1989).

Cell Lines and Transfection

The human kidney epithelial cell line, tsA201 (gift from Dr. J. Kyle, University of Chicago, Chicago, IL), were maintained in DMEM supplemented with 10% calf serum (Hyclone). Cells were transiently transfected with the subunit cDNA constructs using a calcium phosphate protocol (Claudio, 1992). The PC12 cell isolate, N21, was a gift from Dr. Richard W. Burry (Ohio State University, Columbus, OH) and was cultured in DMEM supplemented with 10% fetal bovine serum and 5% heat inactivated horse serum. SH-SY5Y human neuroblastoma cells, stably transfected with the rat α7 subunit cDNA (Puchacz et al., 1994), were a generous gift from Dr. R. Lukas (Barrow Neurological Institute, Phoenix, AZ). Cells were maintained in the same medium as PC12 cells, with the addition of 400 μg/ml of hygromycin B.

Cell-surface ^{125}I-Protein A and Bgt Binding

2 d after transfection, tsA201 cells from 6-cm cultures were removed from the plates and washed with PBS. Under our culture conditions in which the cells were not grown on any substrate, the transfected tsA201 cells were poorly adherent. This property allowed the cells to be gently removed from the plates and transferred into Eppendorf tubes. To estimate levels of α7 and α7/5HT$_3$ subunit expression, the transfected cells were incubated with the anti-HA antibody, mAb 12CA5, in PBS containing 0.1% BSA overnight at 4°C. mAb 12CA5 was harvested from hybridoma supernatant and concentrated on a protein G–Sepharose (Pharmacia) column. Cells were washed with cold PBS and centrifuged (5,000 *g*, 15 s) 3 times to remove unbound antibodies, and then incubated with 0.5 μCi per plate of ^{125}I-protein A (Amersham) in cold PBS-0.1% BSA solution for 3 h at 4°C. Unbound radioactivity was removed by three washes in cold PBS and the samples were counted in a Wallac 1470 gamma counter. To bind cell-surface subunit receptors with Bgt, PC12 cells or cells transfected with α7/5HT$_3$ were incubated with 12.5 nM cold Bgt (Biotoxins Inc.) for 2 h, and washed with cold PBS and centrifuged (5,000 *g*, 15 s) 3 times to remove unbound Bgt.

Metabolic Labeling, Immunoprecipitation, and Immunoblot Analysis

15 h after transfection, 6 cm cultures were starved in methionine-free DMEM for 10–15 min and labeled in methionine-free DMEM containing 100 μCi/ml of an [^{35}S]methionine [^{35}S]cysteine mixture (NEN EXPE^{35}S^{35}S) for the specified times. To follow the subsequent changes in the labeled subunits, the cells were chased by incubation for the indicated times in medium at 37°C. Cells that were chased were washed twice with DMEM supplemented with 5 mM cold methionine and incubated at 37°C in complete medium for the duration of the chase. Cells were then transferred from the plates into Eppendorf tubes, washed twice with PBS, and solubilized in lysis buffer (150 mM NaCl, 5 mM EDTA, 50 mM Tris, pH 7.4, 0.02% NaN_3) containing 2 mM phenylmethylsulfonyl fluoride, 10 μg/ml each of chymostatin, leupeptin, pepstatin and tosyl-lysine chloromethyl ketone, and 1% Triton X-100. Lysates were clarified by centrifugation at 10,000 *g* for 30 min at 4°C, and the supernatants precleared by incubation with Sepharose 4B (Pharmacia) overnight at 4°C. The resin was removed by centrifugation and the supernatant was rotated overnight at 4°C with either saturating amounts of the anti-HA antibody, mAb 12CA5, or Bgt-Sepharose. Bgt-Sepharose was prepared by coupling Bgt to CNBr-activated Sepharose 4B (Pharmacia) according to the manufacturer's directions. The receptor-antibody complex was precipitated with protein G–Sepharose. The resin was washed twice in lysis buffer similar to the one used above, but with 500 mM NaCl instead of 150 mM and addition of 0.1% SDS, and twice with regular lysis buffer. Precipitates were eluted from the beads with gel loading buffer and separated on 4–8% gradient SDS-PAGE with the exception of the truncated α7 construct where 10% SDS-PAGE was used (see Fig. 3 D). Gels were stained, fixed, treated with

Amplify (Amersham) for 30 min, dried, and exposed to Kodak XRP film at −70°C with intensifying screens.

For immunoblots, confluent 10 cm cultures of PC12 and the SH-SY5Y cells were treated, solubilized, and subunits precipitated with Bgt-Sepharose as described above. PC12 cell-surface receptors bound with Bgt were immunoprecipitated with anti-Bgt antibodies coupled to protein A–Sepharose. Precipitates were eluted from the beads with gel loading buffer and separated on 4–8% gradient SDS-PAGE. Proteins separated by SDS-PAGE were electrophoretically transferred to nitrocellulose membrane (Towbin et al., 1979) in a Hoefer transfer unit. After transfer, the nitrocellulose was treated with 3% BSA in wash buffer (10 mM Tris, pH 7.4, 0.05% Tween 20, 150 mM NaCl), washed briefly in the wash buffer, and then incubated with the primary antibody in wash buffer containing 0.3% BSA for 1 h at room temperature. Membranes were first probed with C-20 (Santa Cruz Biotechnology), an anti–α7 polyclonal antibody (1:1,000 dilution). The membrane was washed and incubated by rabbit anti–goat-HRP antibody (at 1:100,000 dilution), and then treated with an enhanced chemiluminescent reagent (ECL, Amersham) according to the manufacturer's protocol and exposed to Kodak XLS film.

Immunofluorescence Staining

Live, intact cells were stained with an α-bungarotoxin tetramethylrhodamine conjugate (TMR-Bgt) used at 300 nM (Molecular Probes) and a mouse monoclonal anti-HA antibody used at 1:1,000 (BAbCO). The secondary antibody (used at 1:500) was an affinity-purified fluorescein isothiocyanate conjugated goat anti–mouse immunoglobin (Molecular Probes). Nuclei were stained with DAPI (Molecular Probes). Transiently transfected cells were immobilized on Alcian blue (Eastman Kodak) coated slides, fixed with 2% paraformaldehyde (Sigma), and preblocked with TBS supplemented with 2 mg/ml BSA (Sigma), TBS/BSA. Primary and secondary Abs, as well as TMR-Bgt, were diluted in TBS/BSA and allowed to react with cells for 1 h at room temperature. After each incubation, cells were rinsed 3 times, 5–10 min each time, with TBS/BSA. Cells were mounted in Vectashield (Vector Laboratories), viewed, and photographed with a Zeiss Axioplan microscope using a 100× 1.4 NA Plan Apo objective.

Electrophysiology

Cells expressing α7 or α7/5HT$_3$ on their surface were visualized by means of an inverted microscope equipped with epifluorescence illumination and Hoffman optics (Zeiss Axiovert 135). Membrane currents were measured with the whole-cell configuration of the patch clamp technique (Hamill et al., 1981) using an Axopatch 200B amplifier (Axon Instruments). The criterion for adequate electrical access was 10 MΩ or less, as determined by the compensation circuitry of the patch clamp. The pipette solution included (mM) 140 K-gluconate, 10 KCl, 1 EGTA, 5 K-ATP, 10 Hepes, 10 glucose, pH, 7.4. The external solution included (mM) 145 NaCl, 2.5 KCl, 1 $MgCl_2$, 1 $CaCl_2$, 10 glucose, 10 Hepes, pH, 7.4. Nicotine was applied by means of a perfusion system with a solution exchange time from 20–100 ms and experiments were carried out at 22–24°C. Membrane currents were digitized and analyzed using a microcomputer (Dell Pentium 200 MHz) equipped with a Digidata 1200 A/D interface and PClamp 6.0 software (Axon Instruments).

Results

Cell-surface α7 Subunits That Do Not Bind Bgt

Heterologous expression of α7 subunits in many different cell lines results in little to no expression of Bgt-binding sites (Cooper and Millar, 1997; Rangwala et al., 1997). In contrast, expression of a chimeric subunit, composed of the extracellular NH_2-terminal half of the α7 subunit and the COOH-terminal half of the 5HT$_3$ subunit, produces high levels of Bgt-binding sites (Corringer et al., 1995; Rangwala et al., 1997). To address whether α7 subunits lacking Bgt-binding sites arrive at the surface of cells, we generated a fusion protein of the α7 subunit with a HA epitope tag on the COOH terminus (α7-HA). The same HA epitope tag was also fused to the COOH terminus of the α7/5HT$_3$ chimeric subunit. As illustrated in Fig. 1 A, the HA epitope was expected to have an extracellular location, given the predicted membrane topology. Intact cells expressing α7/5HT$_3$-HA subunits were intensely stained by the anti-HA mAb (Fig. 1 B), and we conclude that the HA epitope and the COOH terminus of the α7/5HT$_3$-HA subunits are located in the extracellular domain of the receptor. Transient transfection of α7/5HT$_3$-HA subunits in tsA201 cells results in expression in ∼50% of the cells as determined by comparing DAPI nuclei staining (Fig. 1 B, left panels) with the anti-HA mAb staining. Consistent with Bgt binding to these receptors, all cells stained by the anti-HA mAb were also highly stained by TMR-Bgt (Fig. 1 B, middle panels).

In light of earlier findings that expression of α7 subunits does not produce Bgt-binding sites, it was surprising that large numbers of the cells transfected with the α7-HA subunit stained positive with the anti-HA mAb (Fig. 1 B). As expected, no cells stained positive with TMR-Bgt. Thus, α7-HA subunits on the surface of these cells lack Bgt-binding sites. The relative amounts of cell-surface α7-HA and α7/5HT$_3$-HA subunits were determined using the anti-HA mAb and ^{125}I-protein A. Fig. 1 C illustrates that α7/5HT$_3$-HA subunit expression was sixfold higher than α7-HA subunit expression. The reason for the difference in the levels of surface expression is unclear, but it is not caused by differences in rates of α7-HA and α7/5HT$_3$-HA subunit synthesis (see Figs. 3 and 4).

Surface α7 Subunit Complexes Are Nonfunctional

Since significant numbers of α7 subunits are transported to the surface of transfected cells, we examined whether these subunits form functional receptors. We tested the nicotine sensitivity of tsA201 cells transfected with the α7/5HT$_3$-HA construct and stained with the anti-HA antibody. In whole-cell voltage clamp recordings, 15 of 15 cells responded to nicotine with robust inward currents that desensitized in the continued presence of the agonist, as expected for an AChR-mediated response (Fig. 2 A). In the same cultures, cells that did not stain positive with the anti-HA antibody did not respond to nicotine application (n = 12; not shown). In contrast to the cells expressing α7/5HT$_3$-HA, the application of nicotine to α7-HA–transfected cells that stained with anti-HA antibody, did not elicit any response (n = 11; Fig. 2 B). These findings indicate that the α7-HA subunit complexes expressed on the surface of these cells do not form functional receptors.

Differences in α7 and α7/5HT$_3$ Subunit Redox State

To identify the basis for the differences between α7-HA and α7/5HT$_3$-HA subunits, we performed a series of experiments that compared the processing of the two subunits. For the muscle-type AChR, formation of the Bgt-binding site requires disulfide bonding of two cysteine residues in the extracellular, NH_2-terminal domain of the α1 subunit (Mishina et al., 1985; Sumikawa and Gehle, 1992; Green and Wanamaker, 1997). Because a homologous set of cysteine residues is found on the extracellular, NH_2-terminal domain of α7 and α7/5HT$_3$ subunits, we tested whether the subunits differ in their redox state. If

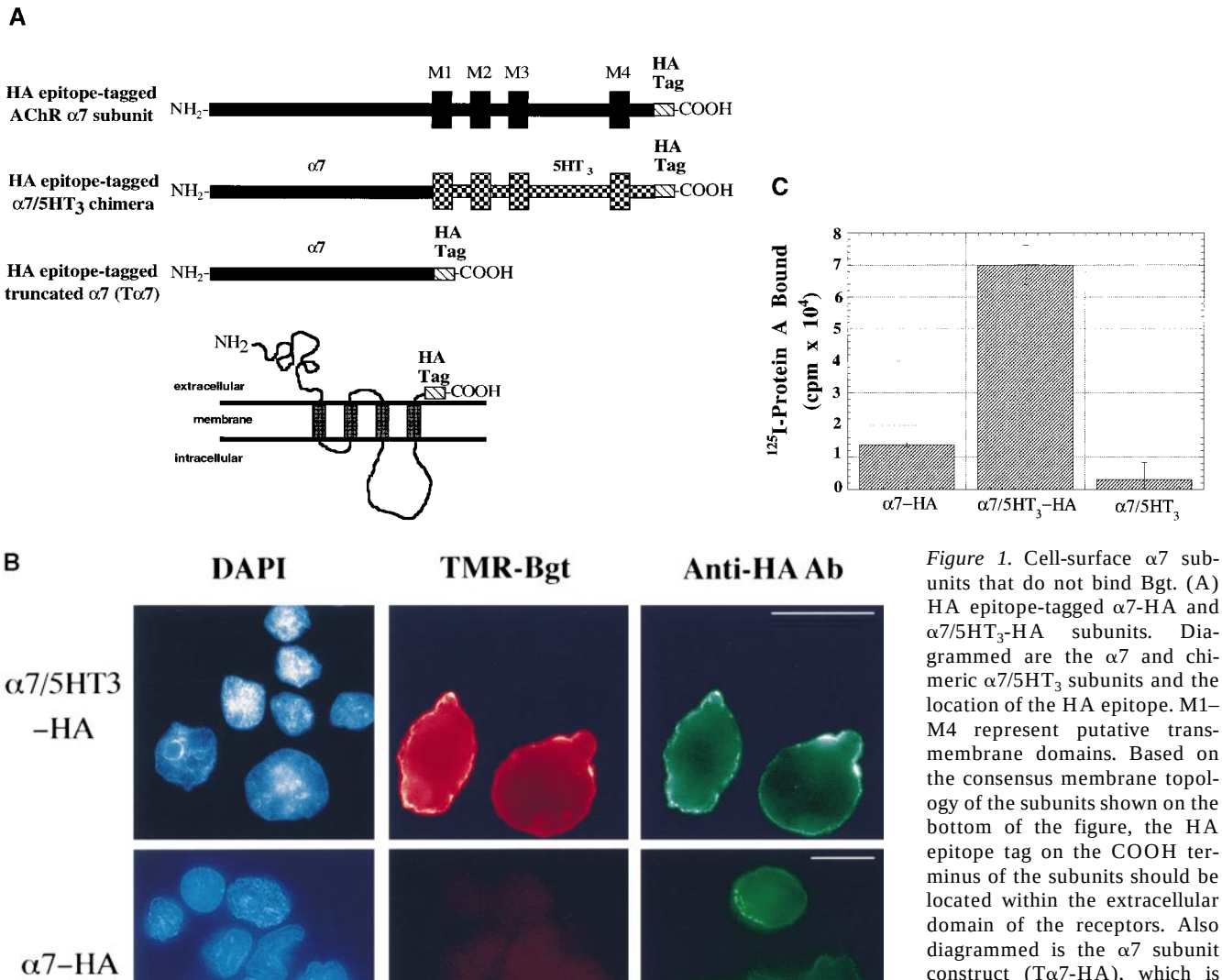

Figure 1. Cell-surface α7 subunits that do not bind Bgt. (A) HA epitope-tagged α7-HA and $\alpha7/5HT_3$-HA subunits. Diagrammed are the α7 and chimeric $\alpha7/5HT_3$ subunits and the location of the HA epitope. M1–M4 represent putative transmembrane domains. Based on the consensus membrane topology of the subunits shown on the bottom of the figure, the HA epitope tag on the COOH terminus of the subunits should be located within the extracellular domain of the receptors. Also diagrammed is the α7 subunit construct (Tα7-HA), which is truncated just before the first transmembrane domain (M1) and also contains the HA epitope tag at the COOH terminus. (B) Immunostaining of $\alpha7/5HT_3$-HA and α7-HA subunits on the cell surface. TsA201 cells, transfected with either $\alpha7/5HT_3$-HA or α7-HA cDNA constructs, were immobilized on slides and immunostained using an anti-HA mAb. Photographs were taken sequentially in the same field after staining with a nuclear stain, DAPI (blue), TMR-Bgt (red), and anti-HA mAb complexed with fluorescein-conjugated secondary Ab (green). DAPI staining is included to stain untransfected as well as transfected cells. Bar, 10 μm. Note the difference in scale. The cells expressing $\alpha7/5HT_3$-HA were photographed with a 100× objective whereas those expressing α7-HA were photographed with a 63× objective. (C) ^{125}I-protein A binding to surface $\alpha7/5HT_3$-HA and α7-HA subunits. TsA201 cells were transiently transfected with either α7-HA, $\alpha7/5HT_3$-HA, or $\alpha7/5HT_3$ cDNA in 6-cm plates. To compare subunit surface expression levels 48 h after transfection, cells were incubated with saturating concentrations of anti-HA mAb and ^{125}I-protein A, and specific binding was determined. Each bar represents the mean of three determinations ± SD.

the alkylating agent, *N*-ethylmaleimide (NEM), is not present during solubilization of the labeled subunits, the migration of α7 subunits on nonreducing gels was distinct from $\alpha7/5HT_3$ subunits (Fig. 3 A, lanes 1 and 2). Under these conditions, none of the metabolically labeled α7 subunits migrated at the expected position of ~60 kD (Couturier et al., 1990; Schoepfer et al., 1990). Instead, α7 subunits migrated as aggregates, i.e., in a broad mass at much higher molecular weights. Metabolically labeled $\alpha7/5HT_3$ subunits, in contrast, migrated at the expected molecular weight of an ~60-kD monomer, although some of the labeled $\alpha7/5HT_3$ subunits also migrate as aggregates. The differences in the migration of labeled $\alpha7/5HT_3$ and α7 subunits under these conditions indicate that the two subunits differ in their redox state.

Subunit aggregation is caused by disulfide bonding of the subunits since no α7 or $\alpha7/5HT_3$ subunit aggregates are observed on reducing gels (Fig. 3 A, lanes 3 and 4), and

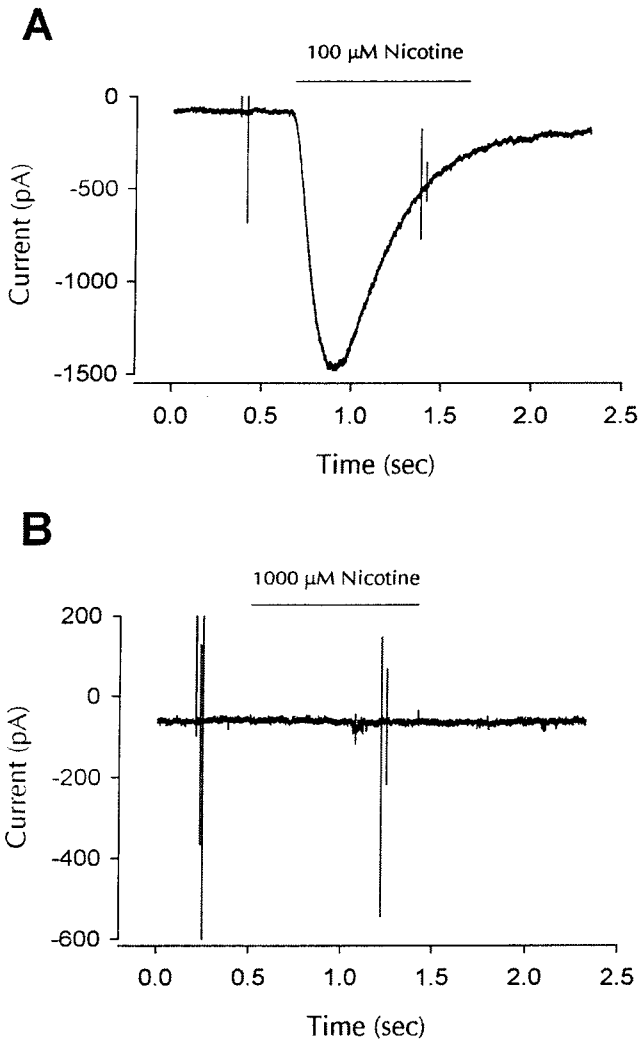

Figure 2. α7 subunit complexes are nonfunctional. (A) Whole-cell response to nicotine for cells expressing α7/5HT$_3$-HA subunits. α7-5HT$_3$-HA transfected cells were identified by positive staining with anti-HA mAb, and whole cell patch clamp recordings showed functional nicotine-gated currents at a potential of −70 mV (100 μM nicotine; similar responses were seen in 15 of 15 cells). No responses were seen in cells that were not positively stained with the anti-HA mAb (n = 12). (B) Whole-cell response to nicotine for cells expressing α7-HA subunits. Transfection with α7-HA results in positive staining of live cells, but no inward currents were seen at holding potentials of −70 mV. In total, 11 cells were exposed to a 10-fold higher nicotine concentration (1 mM). Except for their response to nicotine, cells expressing α7-HA subunits appeared to be identical to cells expressing α7/5HT$_3$-HA subunits.

the subunits run predominantly as monomers at ~60 kD. The very broad distribution of the aggregates on nonreducing gels further suggests that the subunits are disulfide bonded randomly to other proteins, as well as to each other. Surprisingly, aggregation of α7 subunits was prevented if NEM was added during solubilization of the subunits (Fig. 3 C) or even if intact cells were briefly exposed to NEM concentrations as low as 100 μM before solubilization (Fig. 3 B). For alkylation to prevent disulfide-linked subunit aggregation, α7 subunits must contain free sulfhydryl groups that can be alkylated before subunit aggregation. Because subunit aggregates are prevented by subunit alkylation, we conclude that aggregates are absent in vivo and must form during solubilization. Furthermore, the α7 subunit free sulfhydryl groups that can be alkylated in intact cells are somehow prevented from forming disulfide bonds, and this obstacle is removed during solubilization. Aggregation of the α7/5HT$_3$ subunits, which occurred to a lesser extent than the aggregation of α7 subunits (Fig. 3 A), was also prevented by alkylation of the subunits with NEM (Figs. 3 D and 4 B).

In addition to aggregates and subunit monomers on the gels, α7 and α7/5HT$_3$ subunits ran as a ladder of higher molecular weight bands where each rung was a multiple of the monomer (Fig. 3, A, C, and D). Bands corresponding to subunit dimers, trimers, tetramers, and pentamers were observed, but there were no complexes larger than pentamers (see Figs. 4–6). These data are consistent with α7 subunits complexing into pentamers, similar to α7/5HT$_3$ subunit receptors (Rangwala et al., 1997) and other characterized AChRs (Karlin and Akabas, 1995). For α7 subunits, a large number of the multimers was present even on reducing gels or alkylated with NEM, though alkylation did disperse some of the larger multimers (Fig. 3 C). Since most of the α7 multimers remained tightly associated even in the presence of SDS, they must be held together by SDS-resistant associations in addition to any disulfide bonds. α7/5HT$_3$ subunit multimers were also observed and most remained intact on reducing gels or after NEM alkylation (Figs. 3 A and 4 B). These SDS-resistant associations between subunits are similar to those observed for other oligomeric proteins such as K^+ channel subunits (Cortes and Perozo, 1997). α7/5HT$_3$ subunit multimers, precipitated with Bgt-affinity resin, were dispersed after NEM alkylation and reduction (Fig. 3 D). Thus, there was a loss of the SDS-resistant subunit associations after Bgt-binding sites appeared on α7/5HT$_3$ subunits.

A similar set of experiments was performed using an α7 subunit construct truncated just before the first transmembrane domain (Tα7-HA; Fig. 1 A). These truncated α7 subunits assemble into pentameric complexes, and a small percentage of the subunits binds both Bgt and agonists (Wells et al., 1998). The truncated subunits were metabolically labeled after transient expression in tsA201 cells and immunoprecipitated with the anti-HA mAb. In several respects, the redox state of the truncated subunits was similar to that of the full-length α7 subunits under similar conditions. On nonreducing gels in the absence of NEM alkylation, most of the truncated subunits migrated as aggregates (Fig. 3 E, lane 1). With or without NEM in the solubilizing buffer, subunit multimers corresponding to truncated subunit monomers through pentamers were observed (Fig. 3 E, lanes 1 and 2; Fig. 3 F). Since both the truncated subunit aggregates and multimers were absent on reducing gels (Fig. 3 E, lane 3), the aggregates and multimers resulted from disulfide bonds between the subunits. The ability of the truncated α7 subunits to form disulfide-bonded aggregates and multimers similar to the full-length α7 subunits indicates that the disulfide bonding occurs between the extracellular NH_2-terminal domains of the subunits. It should also be noted that there were differences between the truncated and full-length α7 subunits. On

nonreducing gels in the absence of NEM alkylation, some truncated subunits migrated as monomers. In addition, the truncated subunit multimers totally disappeared on reducing gels (Fig. 3 E, lane 3), and thus, did not display the SDS-resistant associations of the full-length α7 subunits.

Disulfide Bond Formation and the Change in α7/5HT$_3$ Subunit Redox State

Although subunit aggregates are artifacts of solubilization, their appearance can be used as an assay of the α7 and α7/5HT$_3$ subunit redox state. Cells expressing either subunit were briefly metabolically labeled and the redox state of the subunits was assayed at different times after labeling (Fig. 4, A and B). Immediately following subunit synthesis, α7 subunits were in a state that resulted in subunit aggregates during solubilization and remained in that state after synthesis (Fig. 4 A). Virtually all of the α7/5HT$_3$ subunits were also in aggregates on the gels following their synthesis (Fig. 4 B, second gel, lane 2). However, unlike

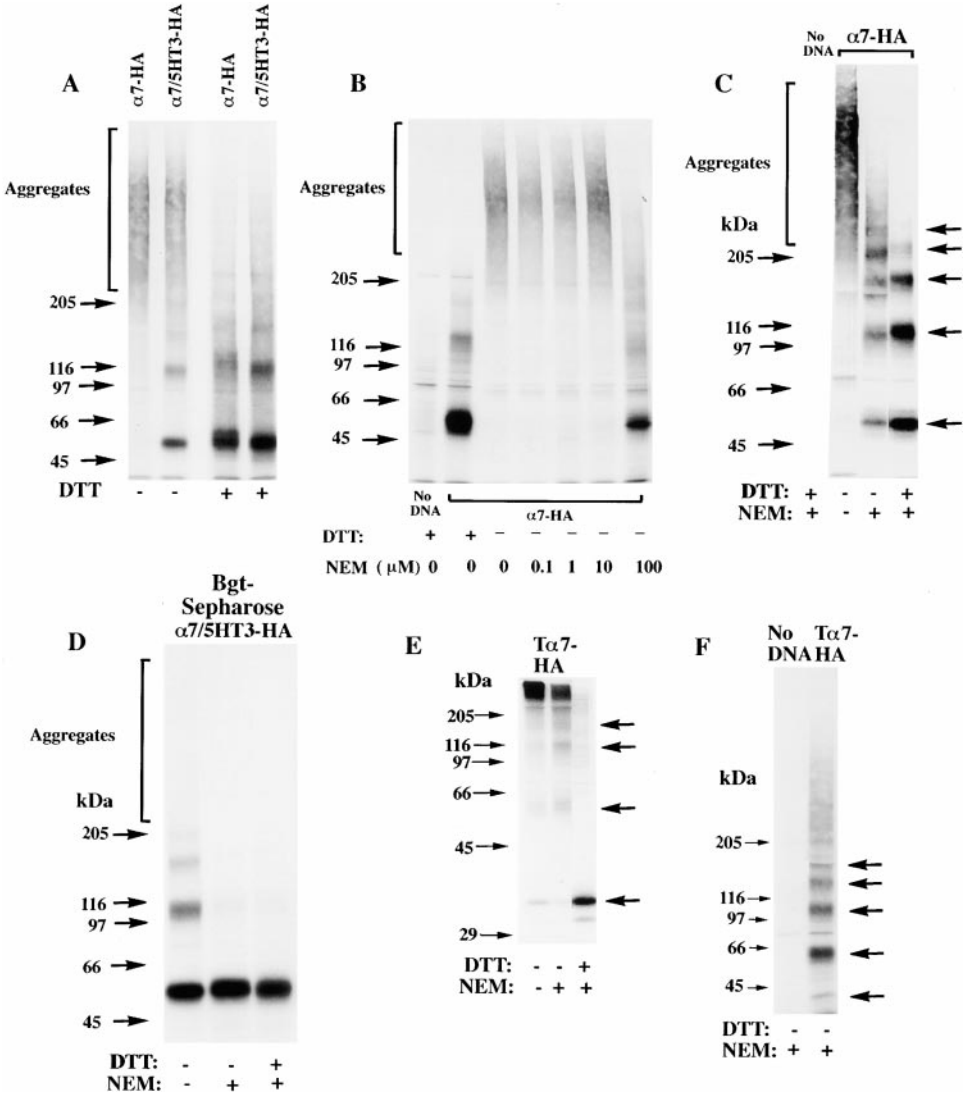

Figure 3. Differences in the folding of α7-HA and α7/5HT$_3$-HA subunits. (A) A difference in α7 and α7/5HT$_3$ subunit redox state. 6-cm cultures of tsA201 cells, transfected with α7-HA or α7/5HT$_3$-HA cDNAs, were metabolically labeled for 1 h and chased for 1 h. The cells were solubilized in the absence of NEM and labeled subunits immunoprecipitated with anti-HA mAb. Samples, each from one 6-cm culture, were loaded on the gel with or without treatment with 10 mM DTT. α7-HA samples were loaded into lanes 1 and 3 and α7/5HT$_3$-HA samples were loaded into lanes 2 and 4. Arrows on the left of the figure are the indicated molecular weight markers run on a separate lane. Arrows on the right of the figure indicate positions of monomer, dimer, trimer, tetramer, and pentamer subunit complexes. (B) α7 subunit alkylation prevents its aggregation. TsA201 cells were transfected with α7-HA cDNA, metabolically labeled, and precipitated as in A, except that NEM (0–100 μM) was included in the culture medium for the final 10 min of the chase. A sample from sham-transfected cells (no DNA) was run in lane 1. Arrows on the left and right of the figure are the same as in A. (C) SDS resistance of subunit multimers. TsA201 cells were transfected with α7-HA cDNA, metabolically labeled, and precipitated as in A. As indicated, NEM (2 mM) was added to the solubilization buffer and to the loading buffer after addition of DTT (1 mM). After alkylation by NEM (lane 3) and reduction by DTT before gel loading (lane 4), some subunits remained in complexes as well as migrating as monomers. Arrows on the left of the figure are the indicated molecular weight markers run on a separate lane. Arrows on the right of the figure indicate positions corresponding to monomer, dimer, trimer, tetramer, and pentamer subunit complexes. (D) Bgt-binding subunit multimers. TsA201 cells transfected with α7/5HT$_3$-HA cDNA were metabolically labeled as in A, chased for 2 h, and subunits precipitated with Bgt-Sepharose. Subunit multimers were greatly decreased by NEM alkylation (2 mM; lane 2) and addition of DTT before gel loading (1 mM; lane 3). A sample from sham-transfected cells (no DNA) was run in lane 1. Molecular weight markers are on the left of the gel. (E and F) The truncated α7 subunit. TsA201 cells were transfected with the truncated α7 subunit cDNA (Tα7-HA; Fig. 1 A), metabolically labeled, and immunoprecipitated as in A. Labeled subunits were analyzed on 10% (E) or 4–8% gradient (F) gels. As indicated, NEM (2 mM) was added to the solubilization buffer and to the loading buffer after addition of DTT (1 mM). Truncated α7 subunits migrated as aggregates and multimers similar to full-length α7 subunits (A–C). Arrows on the left of the figures are the indicated molecular weight markers run on a separate lane. Arrows on the right of the figures indicate positions corresponding to monomer, dimer, trimer, and tetramer (E and F) plus pentamer (F) subunit complexes.

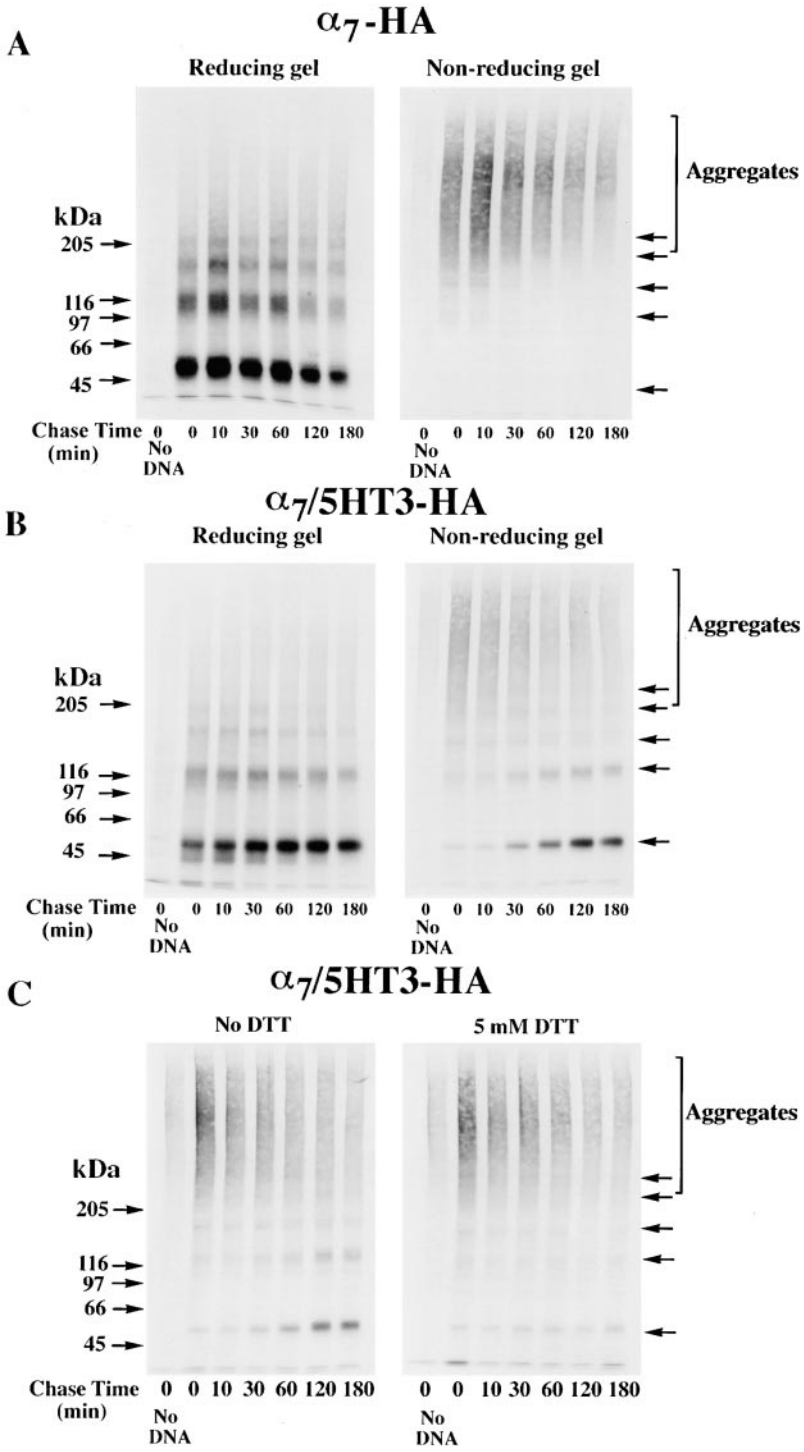

Figure 4. Disulfide bonding is required to effect a change in $\alpha7/5HT_3$ subunit redox state. (A and B) Time-dependent change in $\alpha7/5HT_3$-HA subunit redox state. TsA201 cells transfected with α7-HA (A) or $\alpha7/5HT_3$-HA (B) cDNAs were metabolically labeled for 10 min and chased for the times specified in the figure. The cells were solubilized in the absence of NEM, labeled subunits immunoprecipitated with anti-HA mAb, and samples loaded on the gels without (nonreducing) or with (reducing) 10 mM DTT. A sample from sham-transfected cells (no DNA) was run in lane 1 of each of the four gels. Arrows on the right of the figure indicate positions of putative monomer, dimer, trimer, tetramer, and pentamer $\alpha7/5HT_3$-HA subunit complexes. (C) Addition of 5 mM DTT to the cell medium blocks the redox state change. TsA201 cells transfected with $\alpha7/5HT_3$-HA cDNA were metabolically labeled for 10 min and chased for the times specified in the figure in the absence (left) or presence (right) of 5 mM DTT in the medium. Cells were solubilized in the absence of NEM and labeled subunits precipitated with anti-HA mAb. All samples were loaded on the gels without DTT, and a sample from sham-transfected cells (no DNA) was run in lane 1 (left and right). Arrows on the right of the figure indicate positions of putative monomer, dimer, trimer, tetramer, and pentamer $\alpha7/5HT_3$-HA subunit complexes.

the α7 subunits, a small fraction of the $\alpha7/5HT_3$ subunits appeared as monomers on the gel and thus were in the different redox state. The number of $\alpha7/5HT_3$ subunit monomers increased with time whereas the number of subunit aggregates decreased until most of the $\alpha7/5HT_3$ subunits migrated as monomers. Based on these results, we conclude that α7 and $\alpha7/5HT_3$ subunits are in a similar redox state immediately following subunit synthesis. The differences observed between these subunits arise over time and are caused by processing events that convert $\alpha7/5HT_3$ subunits from the redox state where subunits are aggregated to the state where the subunits migrate as monomers on the gels.

To test whether disulfide bonds form on $\alpha7/5HT_3$ subunits during the change in subunit redox state, the reducing agent, DTT, was applied to the cells after metabolically labeling the subunits (Fig. 4 C). When added to the medium of cultures, DTT permeates cells and prevents the formation of protein disulfide bonds in the ER as well as reduces existing disulfide bonds without altering most

other cellular functions (Braakman et al., 1992). After the addition of 5 mM DTT, the $\alpha 7/5HT_3$ subunits remained as aggregates on the gels and all subsequent conversion to monomers was blocked (Fig. 4 C). Note that the small number of monomers observed in Fig. 4 C exist during the pulse when no DTT was present and do not increase after the addition of DTT. Therefore, addition of 5 mM DTT to the cell medium after the subunits were labeled prevented the change in $\alpha 7/5HT_3$ subunit redox state. The effect of DTT was reversible. If the DTT was removed from the medium, $\alpha 7/5HT_3$ subunit aggregates again converted into the monomeric $\alpha 7/5HT_3$ subunit conformation with time (data not shown). Based on these data, we conclude that disulfide bonds form on $\alpha 7/5HT_3$ subunits during the change in subunit redox state. The $\alpha 7/5HT_3$ subunits, which result from the redox state change, migrate as subunit monomers on nonreducing gels with the exception of the subunit multimers that form during solubilization in the absence of subunit alkylation (see Fig. 3 D). The disulfide bonds that form during the redox state change, thus, are intrasubunit bonds.

Bgt-binding Site Formation Coincides with the Change in $\alpha 7/5HT_3$ Subunit Redox State

Since Bgt-binding sites form on $\alpha 7/5HT_3$ subunits and not on $\alpha 7$ subunits (Fig 1 B; Cooper and Millar, 1997; Rangwala et al., 1997), we tested whether Bgt-binding site formation correlates with the change in $\alpha 7/5HT_3$ subunit redox state. To monitor Bgt-binding site formation, equal aliquots of labeled $\alpha 7/5HT_3$ subunits were precipitated using Bgt-Sepharose or with the anti-HA mAb at different times after subunits were labeled (Fig. 5 A). A strong correlation exists between the appearance of Bgt-Sepharose

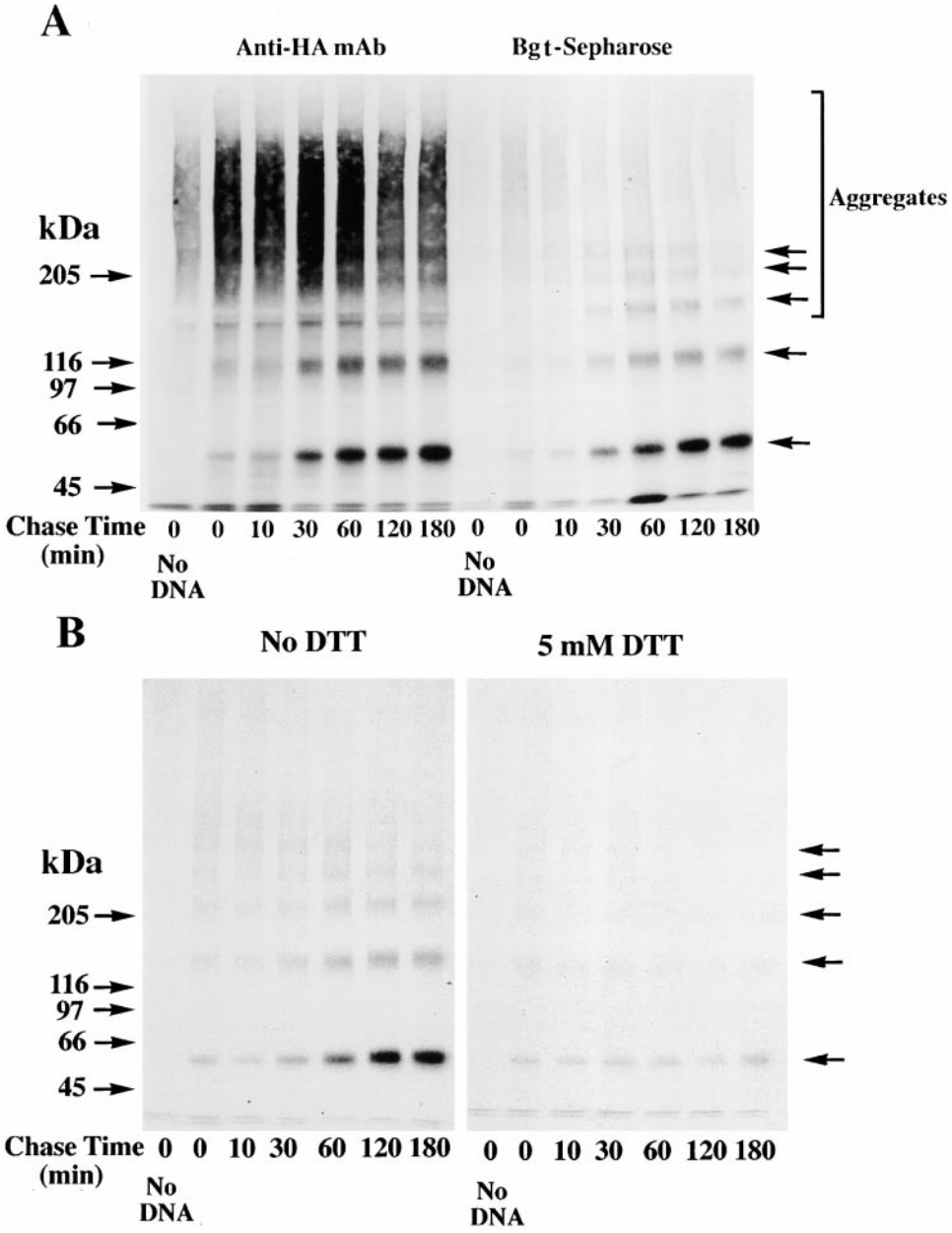

Figure 5. Bgt-binding site formation and the change in redox state. (A) Formation of Bgt-binding site correlates with the change in redox state. TsA201 cells transfected with $\alpha 7/5HT_3$-HA cDNA were metabolically labeled for 10 min and chased for the times specified in the figure. The cells were solubilized in the absence of NEM and labeled subunits precipitated with anti-HA mAb (lanes 2–7 on the left) or Bgt-Sepharose (lanes 2–7 on the right). Bgt-Sepharose appeared not to precipitate all of the $\alpha 7/5HT_3$ subunit monomers precipitated by anti-HA mAb. It is possible that not all $\alpha 7/5HT_3$ subunit monomers assemble into Bgt-binding complexes or, alternatively, Bgt-Sepharose fails to quantitatively precipitate all Bgt-binding sites. All samples were loaded on the gels without DTT, and a sample from sham-transfected cells (no DNA) was run in lane 1 (left and right). Arrows on the right of the figure indicate positions of putative monomer, dimer, trimer, tetramer, and pentamer $\alpha 7/5HT_3$-HA subunit complexes. (B) Addition of 5 mM DTT to the cell medium blocks Bgt-binding site formation. The experiment was performed as in Fig. 4 C except that labeled subunits were precipitated with Bgt-Sepharose.

precipitated subunits and the change in subunit redox state as assayed by subunit monomers precipitated with the anti-HA mAb. Bgt-Sepharose precipitated almost all $\alpha7/5HT_3$ subunit monomers and smaller amounts of $\alpha7/5HT_3$ subunit aggregates. Furthermore, the time course of Bgt-binding site formation and appearance of $\alpha7/5HT_3$ subunit monomers is indistinguishable.

We also tested whether Bgt-binding site formation is blocked by the addition of DTT after subunit labeling. Again, 5 mM DTT was added to the medium of cells in which $\alpha7/5HT_3$ subunits were labeled. The presence of the DTT blocked the formation of Bgt-binding sites as shown by the absence of additional Bgt-Sepharose precipitated subunits after DTT was applied to the medium (Fig. 5 B). Therefore, intrasubunit disulfide bonding of $\alpha7/5HT_3$ subunits is also required for Bgt-binding site formation. Clearly, Bgt-binding site formation and the redox state change are closely linked events during $\alpha7/5HT_3$ receptor assembly as shown by the block of both events by DTT and their close correlation in time.

$\alpha7$ and $\alpha7/5HT_3$ Bgt-binding Complexes Contain Subunits in Different Redox States

Although there is a strong correlation between the appearance of subunit monomers on gels and the formation of Bgt-binding sites, Bgt-Sepharose also precipitated subunit aggregates and multimers (Figs. 5 A and 3 D). This finding indicates that Bgt-binding $\alpha7/5HT_3$ receptors contain $\alpha7/5HT_3$ subunits in both redox states. To further test whether both conformations are present within a receptor, we isolated surface Bgt-binding $\alpha7/5HT_3$ receptors. We had demonstrated previously that the surface receptors are a uniform population of pentamers with a molecular mass of 260 kD and that all receptors cooperatively bound agonist (Rangwala et al., 1997). Intact cells were bound with cell-impermeant Bgt, and the Bgt-bound receptors were immunoprecipitated with anti-Bgt antibodies to specifically isolate surface receptors. The labeled subunits were analyzed on nonreducing gels and the subunits solubilized in the absence or presence of NEM were compared (Fig. 6 A). In the absence of NEM, subunit aggregates and multimers were observed along with subunit monomers. When alkylated with NEM, aggregates and multimers were dispersed, which increased the number of subunit monomers on the gel. Since the surface receptors consist of a homogenous population of pentamers, we conclude that surface receptors contain subunits in both redox conformations. The approximately twofold increase in monomers with NEM alkylation further demonstrates that a significant number of $\alpha7/5HT_3$ subunits in Bgt-bound, surface receptors are found in both redox states.

PC12 and SH-SY5Y cell lines were used to look at the processing of $\alpha7$ subunits in cells that produce functional, Bgt-binding $\alpha7$ receptors. The PC12 cells have endogenous Bgt-binding receptors that contain $\alpha7$ subunits (Blumenthal et al., 1997; Rangwala et al., 1997) whereas the SH-SY5Y cells stably express rat $\alpha7$ subunits in addition to endogenous $\alpha7$ subunits (Peng et al., 1994; Puchacz et al., 1994). The $\alpha7$ subunits in these cell lines lack the HA epitope and the level of subunit synthesis is not as high as that achieved by transient transfection. These differences prevented us from characterizing $\alpha7$ subunits in these cell lines to the same degree as the $\alpha7$-HA and $\alpha7/5HT_3$-HA subunits in tsA201 cells. Nonetheless, we were able to precipitate $\alpha7$ subunits from SH-SY5Y and PC12 cells using Bgt-Sepharose and performed Western blot analysis on the $\alpha7$ subunits from both cell lines (Fig. 6, B and C). The processing of $\alpha7$ subunits in SH-SY5Y and PC12 cells was different from that of $\alpha7$ subunits in tsA201 cells. In the absence of NEM alkylation, many $\alpha7$ subunits in these cells migrated as monomers on a nonreducing gel (Fig. 6, B and C, lane 1). Such monomers were never observed on nonreducing gels with the expression of the $\alpha7$-HA subunits in tsA201 cells. In addition to the monomers, there were subunit aggregates and multimers. Like Bgt-binding $\alpha7/5HT_3$ subunits in tsA201 cells (Fig. 3 D), the $\alpha7$ subunit multimers, precipitated with Bgt-affinity resin, were dispersed by NEM alkylation and reduction (Fig. 6, B and C, lane 2). Identical results were found for cell-surface PC12 BgtRs specifically isolated by binding Bgt to intact cells and immunoprecipitating the Bgt-bound receptors with anti-Bgt antibodies (Fig. 6 C, lanes 4 and 5).

$\alpha7$ subunits isolated from SH-SY5Y and PC12 cells differed from $\alpha7$ and $\alpha7/5HT_3$ subunit from tsA201 cells in that the subunits migrated as a doublet after NEM alkylation on reducing gels (Fig. 6 B, lane 2, and C, lanes 2 and 4). Both doublet bands are recognized by $\alpha7$-specific antibodies on the Western blots and thus are different forms of the $\alpha7$ subunit. Under the same conditions, the doublet bands are also observed with the metabolically labeled subunits (data not shown). The lower band of the doublet migrated precisely at the same position as the tsA201-expressed $\alpha7$-HA subunit monomer band (Fig. 6, B and C, lane 3). The lower band, therefore, corresponds to the $\alpha7$ subunit form observed in tsA201 cells, which migrates at this position only when NEM alkylation prevents disulfide aggregation and cross-linking. The upper band migrates slower after alkylation than when it is unalkylated (Fig. 6 B, lane 1, and C, lanes 1 and 5), and it is presumed to be in the second conformational state. It is important to note that the $\alpha7$ subunit doublet was observed under conditions that should eliminate any difference in the redox state of the subunits, i.e., both NEM alkylation and a reducing gel. The presence of two $\alpha7$ subunit bands under these conditions indicates that $\alpha7$ subunits in these cells are distinguished by more than a difference in the redox state of the subunits.

Discussion

$\alpha7$ Subunits Fold into Two Different Conformations

In this study, we have compared the processing of $\alpha7$ and $\alpha7/5HT_3$ subunits in tsA201 cells. $\alpha7/5HT_3$ subunits undergo different time-dependent processing events that include a change in subunit redox state and formation of Bgt-binding sites. These changes were not observed for $\alpha7$ subunits in tsA201 cells, where the subunits assembled into receptors that did not function or bind Bgt. However, $\alpha7$ subunits did undergo the same changes in SH-SY5Y and PC12 cells, where they assembled into functional receptors. After subunit alkylation and reduction, $\alpha7$ subunits from SH-SY5Y and PC12 cells migrated as two

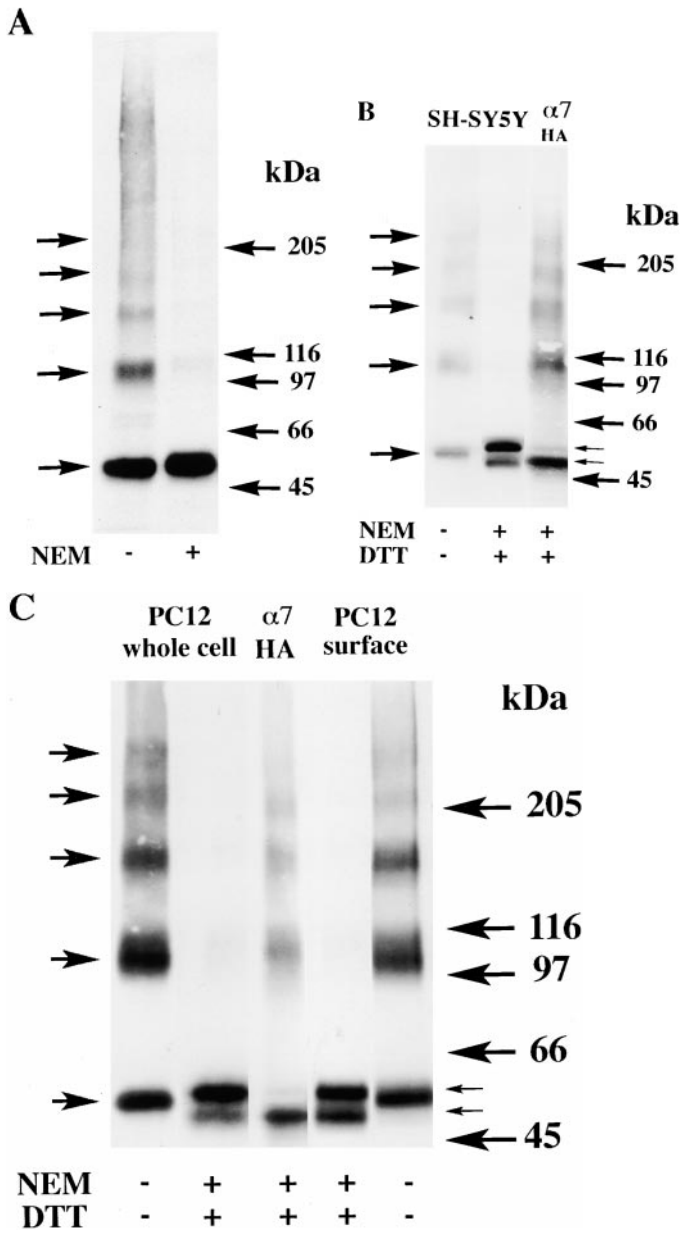

Figure 6. Surface $\alpha7/5HT_3$ and α7 subunit receptors from SH-SY5Y and PC-12 cells contain subunits in two conformations. (A) Surface Bgt-binding receptors contain subunits in different redox states. TsA201 cells, transfected with $\alpha7/5HT_3$-HA cDNAs, were metabolically labeled for 1 h and chased for 2 h. Cells were surface labeled with Bgt and solubilized in the absence (lane 1) or presence (lane 2) of 2 mM NEM. The Bgt-bound receptors were specifically precipitated with anti-Bgt polyclonal antiserum. Arrows on the right of the figure indicate positions of putative monomer, dimer, trimer, tetramer, and pentamer $\alpha7/5HT_3$-HA subunit complexes. (B) α7 subunits expressed in SH-SY5Y cells. α7 subunits stably expressed in SH-SY5Y cells were analyzed by Western blots. Cells were solubilized in the absence (lane 1) or presence (lane 2) of 2 mM NEM and subunits were precipitated using Bgt-Sepharose. The proteins were transferred to a nitrocellulose membrane and probed with the α7 subunit-specific polyclonal antiserum, C-20. Equal samples were loaded on a SDS polyacrylamide gel either directly (lane 1), or preincubated with 1 mM DTT before loading and then treated with 2 mM NEM (lane 2). For lane 3, tsA201 cells were transfected with α7-HA cDNA, metabolically labeled, and precipitated as in Fig. 3 A. The sample was loaded on the same SDS polyacrylamide gel after treatment with 1 mM DTT and then with 2 mM NEM. (C) α7 subunits expressed in PC12 cells. α7 subunits expressed endogenously in PC12 cells were analyzed by Western blots. Cells were solubilized in the absence (lanes 1 and 4) or presence (lanes 2 and 5) of 2 mM NEM. Receptors were either precipitated with Bgt-Sepharose (whole cell; lanes 1 and 2) or cell-surface, Bgt-bound receptors were selectively precipitated with anti-Bgt protein A–Sepharose (surface; lanes 4 and 5). The proteins were transferred to a nitrocellulose membrane and probed with the α7 subunit-specific polyclonal antiserum, C-20. Equal samples were loaded onto an SDS polyacrylamide gel either directly (lanes 1 and 4), or preincubated with 1 mM DTT before loading and then treated with 2 mM NEM (lanes 2 and 5). For lane 3, tsA201 cells were transfected with α7-HA cDNA, metabolically labeled, and precipitated as in Fig. 3 A. The sample was loaded on the same SDS polyacrylamide gel after preincubation with 1 mM DTT and treatment with 2 mM NEM.

separate bands on SDS-PAGE (Fig. 6, B and C). The difference in migration of the two α7 bands appears to be due to differential processing. The α7 subunits in the lower band migrated in the same position as the unprocessed subunits from the tsA201 cells. The α7 subunits in the upper band, thus, correspond to subunits that have undergone the processing that results in the redox state change. Another difference observed for the α7 and $\alpha7/5HT_3$ subunits was that subunit complexes lacking Bgt-binding sites remain associated during SDS-PAGE after reduction and alkylation (Fig. 3, A and C), whereas Bgt-binding complexes were dispersed under the same conditions (Fig. 3 D and Fig. 6). These two differences observed for fully alkylated and reduced subunits, separation into two bands during SDS-PAGE, and the change in subunit associations when exposed to SDS, indicate that subunit processing causes a change more extensive than a difference in redox state.

Surface Bgt-binding $\alpha7/5HT_3$ receptors, surface Bgt-binding α7 receptors from PC12 cells, and Bgt-binding α7 receptors from SH-SY5Y cells all contain significant numbers of subunits in both conformations from which we concluded that each receptor has subunits in two conformations. An alternative interpretation of the data is that there are two independent populations of Bgt-binding receptors, each population with subunits in one of the two conformational states. Several of our findings are inconsistent with this possibility. In tsA201 cells, α7 subunits assemble into pentamers that consist of subunits only in the initial conformation, and these receptors do not bind Bgt. Additionally, Bgt-binding sites on $\alpha7/5HT_3$ subunits appear only as $\alpha7/5HT_3$ subunits change conformation from the first to the second state (Fig. 5 A). It is, therefore, unlikely that there is a population of Bgt-binding receptors with subunits only in the first conformation. Another possible interpretation of the data is that α7 and $\alpha7/5HT_3$ sub-

units are in a single conformation that can form subunit aggregates and multimers, but does so incompletely. If α7 and α7/5HT$_3$ were in such a single conformation, then the relative amounts of subunit aggregates, multimers, and monomers on the gels should not significantly depend on either the time after their synthesis or cell type. However, we found that following subunit synthesis in tsA201 cells, α7/5HT$_3$ subunit aggregation decreased as monomers increased with time. In the same cell line, α7 subunits remained as aggregates, whereas in SH-SY5Y and PC12 cells, all forms of the α7 subunits were observed. Thus, based on all of the data, we conclude that α7 and α7/5HT$_3$ Bgt-binding receptors contain subunits in both conformations. Since only functional receptors contain subunits in the two conformations, both conformations appear to be needed for function.

There is little precedence for our finding that functional α7 subunit receptors contain subunits that are the same gene product folded into different conformations. It is generally assumed that a single, stable conformation is the end result of the folding process of any protein. Protein folding into alternative conformations is usually associated with a pathological state, a good example being prion proteins (Prusiner et al., 1998). Similarly, it has been shown that receptor and ion channel subunits folded into alternative conformations are defective and are rapidly degraded by mechanisms associated with the ER. The ΔF508 mutation of the cystic fibrosis transmembrane regulator (CFTR) ion channel, the most common cause of cystic fibrosis, is not inserted into the plasma membrane. Instead, it is rapidly degraded in the ER because of altered folding that prevents its release from the ER (Cheng et al., 1990). The *Torpedo* AChR subunits expressed in mouse fibroblasts also are not properly folded and are rapidly degraded (Claudio et al., 1989). In both cases, altered folding is a temperature sensitive defect that can be overcome by lowering the temperature (Claudio et al., 1987; Denning et al., 1992). The α7 subunit folding events that lead to the conformational change also appear to occur in the ER. This location is suggested since the conformational change involves intrasubunit disulfide bonding, a processing event that would be expected to occur in the oxidizing environment of the lumen of the ER (Braakman et al., 1991). Also, Bgt-binding site formation of the muscle AChR occurs in the ER (Smith et al., 1987; Gu et al., 1989; Ross et al., 1991) and has a time course very similar to that of the α7/5HT$_3$ subunit receptor (Merlie and Lindstrom, 1983). An important difference between the folding of the α7 subunit and either the mutant cystic fibrosis transmembrane regulator (CFTR) or *Torpedo* AChR subunits is that two different α7 subunit conformations are assembled into functional receptors. Thus, neither α7 subunit conformation is defective, and both α7 subunit conformations are recognized by the cell's quality control mechanisms as properly folded versions of the same gene product.

Disulfide Bonding in the NH$_2$-terminal, Extracellular Domain of the α7 Subunit

Several of our findings together with conserved features of the AChR subunits make it likely that cysteine residues in the subunit's NH$_2$-terminal, extracellular domain are involved in the change in redox state (Fig. 7 A). First, truncated α7 subunits, consisting only of this NH$_2$-terminal, extracellular domain, form disulfide-bonded aggregates and multimers similar to the full-length α7 subunits (Fig. 3, E and F). This finding indicates the free sulfhydryl groups that cross-link the subunits during solubilization are located within this domain. Second, DTT applied to the intact cells prevented the time-dependent change in redox state caused by intrasubunit disulfide bonding of the α7/5HT$_3$ subunits (Fig. 4 C). Based on the membrane topology of α7 and α7/5HT$_3$ subunits (Fig. 7 A), the only cysteines accessible to the ER lumen, and thus available for intrasubunit disulfide bonding, are within the subunit's NH$_2$-terminal, extracellular domain. Moreover, it is only this domain that is shared by α7 and α7/5HT$_3$ subunits, and there is no homology between α7 and 5HT$_3$ subunits with respect to the cysteine residues in the COOH-terminal half of the proteins. Further evidence that the redox state change is caused by disulfide bonding in the subunit's NH$_2$-terminal domain is that the only two disulfide bonds shown to occur on any AChR subunit are located in highly conserved regions within this domain (Fig. 7 A). One of the disulfides is a 15–amino acid cystine loop found on every ACh, 5HT$_3$, γ-aminobutyric acid-A (GABA$_A$), and glycine receptor subunit. The other disulfide is between adjacent cysteines at the ACh-binding site (Kao and Karlin, 1986). For α1 subunits, Bgt site formation requires an intact cystine loop (Mishina et al., 1985; Sumikawa and Gehle, 1992). Bgt site formation does not correlate with the act of forming the disulfide bond, but instead with a subsequent change in α1 subunit conformation which alters antibody accessibility to the loop region (Green and Wanamaker, 1997). If similar events occur for the α7 subunit, a conformational change would help to catalyze formation of the cystine loop on α7 subunits, which, in turn, would promote a conformational change leading to Bgt-binding site formation.

A model of the two α7 subunit conformations is depicted in Fig. 7 A. In the SH state, we envision that cysteine residues in the loop region are buried, preventing oxidation before disulfide bond formation. In the S-S state, the cysteine residues are brought together and become more accessible to the oxidizing ER environment, which catalyzes disulfide bonding. An important feature of this model is that a conformational change occurs that changes the environment of the cysteines before disulfide bonding can occur. α7 subunits differ from virtually every other AChR subunit in that they lack an N-linked glycosylation site consensus sequence within their cystine loop region. Furthermore, compared to α1 subunits, there is an extra cysteine residue within the NH$_2$-terminal domain of α7 subunits. The fifth cysteine residue, at position 112 (Fig. 7 A), is adjacent to an N-linked glycosylation site. A mutation that removes this glycosylation site causes a loss of Bgt-binding site expression in *Xenopus* oocytes, but does not appear to decrease either subunit synthesis or surface expression (Chen et al., 1998). These results raise the possibility that there is no cystine loop between cysteines 128 and 142 in the SH state of the subunit because an alternative cystine between the cysteines 112 and 128 is formed instead.

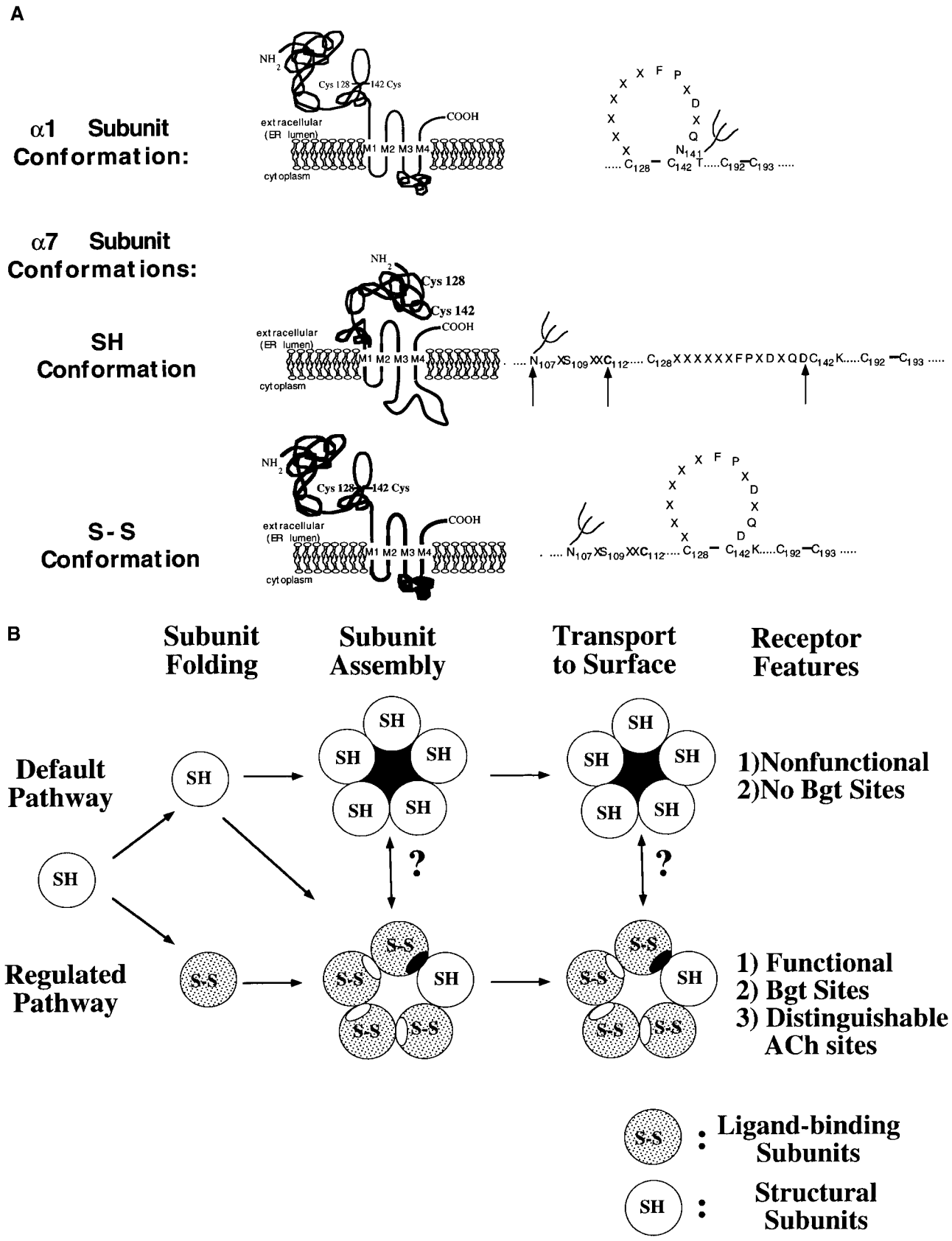

Figure 7. α7 subunits fold and assemble by two different pathways. (A) α7 subunits fold into two conformations. Based on the disulfide bonding of the AChR α1 subunit (Karlin and Akabas, 1995) shown on the top of the figure, a structural interpretation of the α7 subunit redox state change is shown. In the SH conformation, we envision that the 15–amino acid cystine loop is not formed and the two cysteines at residues 128 and 142 are not oxidized. In the S-S conformation, a disulfide bond has formed between these two cysteines. The

The Regulation of α7 Subunit Processing

A consequence of α7 subunit folding into two conformations is that receptors with different properties can be assembled by at least two different pathways. Two such pathways are diagrammed in Fig. 7 B. We have called the path by which α7 subunits assemble when heterologously expressed in most cells the default pathway because the subunits assemble together without additional processing. Along this path, subunits in the SH conformation are assembled into pentamers, presumably in the ER, and the resultant receptors can neither function nor bind Bgt. In SH-SY5Y and in PC12 cells, both the SH and S-S α7 conformations are produced, leading to pentamers that function and bind Bgt. Since assembly along this pathway requires the additional subunit processing that does not occur in certain cells, we have termed this the regulated pathway of assembly. The question marks are included in Fig. 7 B because we have not determined whether the subunits undergo the conformational change before, during, or after assembly into pentamers.

Although neither the Bgt- nor ACh-binding sites lie within the COOH-terminal half of the α7 subunit, this region of the subunit plays a critical role in determining whether receptors bind Bgt and are activated by agonist. In tsA201 cells, receptor function and Bgt binding are only observed when the COOH-terminal half of the α7 subunit is replaced with the COOH-terminal half of the $5HT_3$ subunit. Somehow, the COOH-terminal half of the subunit regulates the conformational state of the subunit's extracellular NH_2-terminal half and determines whether a change in redox state and Bgt-binding site formation can occur. If only the NH_2-terminal half of the α7 subunit is expressed, the truncated α7 subunits undergo the redox state change (Fig. 3 E). This finding further suggests that the α7 subunit COOH-terminal half, in an unmodified state, prevents the conformational change. We can only speculate on the mechanisms that alter the COOH-terminal half of the subunit and, in turn, regulate whether the subunit changes conformation. An attractive hypothesis is that modification of the cytoplasmic domain that lies between the third and fourth membrane spanning regions, regulates the subunit conformation (Fig. 7 A). Within this cytoplasmic domain, there are consensus sequences for different kinds of protein phosphorylation. There is also evidence that proline isomerization of α7 subunits by cyclophilin A is necessary for the expression of functional α7 subunit receptors (Helekar et al., 1994; Helekar and Patrick, 1997). However, there is additional evidence that cyclophilin-mediated proline isomerization is not sufficient to cause expression of Bgt-binding receptors in either HEK 293 cells or PC12 cells (Blumenthal et al., 1997; Cooper and Millar, 1997).

One feature of the regulation of the α7 subunit is that it is cell-type specific. In most cell lines, heterologous expression of α7 subunits results in little to no production of functional receptors or Bgt binding (Cooper and Millar, 1997; Rangwala et al., 1997). Yet, heterologous expression of α7 subunits in cell lines of neuronal or neuroendocrine origin, such as SH-SY5Y cells (Puchacz et al., 1994), PC12 (Blumenthal et al., 1997; Cooper and Millar, 1997), and GH4 cells (Quik et al., 1996), produces functional, Bgt-binding receptors. Note that there are cell lines of neuronal origin in which functional α7 subunit receptors are not expressed (Cooper and Millar, 1997). Furthermore, heterologous expression of Bgt-binding receptors only occurs in PC12 cell isolates where native Bgt-binding sites are found (Blumenthal et al., 1997). Taken together with the findings of this paper, these results suggest that the regulatory mechanisms changing the α7 subunit conformation are restricted to a subset of neurons and neuroendocrine cells, and they act to determine when and where functional, Bgt-binding receptors are produced.

Why are nonfunctional α7 subunit receptors assembled in cells such as the tsA201 cells? One possibility is that the receptors assembled by the default pathway can be transformed into functional receptors, either during transport to the cell surface or after insertion into the plasma membrane. Consistent with this possibility are studies showing that some neuronal AChRs are inserted into the plasma membrane in a nonfunctional state after which the receptors are converted into a functional state (Margiotta et al., 1987; Higgins and Berg, 1988). Another possible explanation is that α7 subunits in the SH conformation can assemble with other AChR subunit isoforms, but that these subunits are absent in the tsA201 cells. Studies indicating that α7 subunits in cultured chick sympathetic neurons can assemble with other AChR subunits support this possibility (Listerud et al., 1991).

α7 Subunit Diversity and Distinguishable ACh-binding Sites

The results of this paper may help to explain how a homomeric receptor can have several ligand-binding sites with distinguishable features. In a recent paper (Rangwala et al.,

arrows mark residues in this region of the α7 subunit that are different from other AChR subunits. These residues are an aspartate at position 141 that replaces an asparagine and removes a conserved consensus site for N-linked glycosylation at residue 141, a fifth cysteine residue at position 112 not found on other AChR α subunits, and an asparagine at residue 107 that creates a consensus site for N-linked glycosylation at residue 107. Our results suggest that changes in the conformation of the NH_2-terminal domain allow the disulfide bonding. The NH_2-terminal domain conformational changes appear to be driven by changes in the conformation of the COOH-terminal half of the subunit, perhaps changes in the COOH-terminal half cytoplasmic domain as depicted in the figure. (B) Assembly of α7 subunit complexes by different pathways. As depicted in the figure, we have found that α7 subunits can fold and assemble into two conformations. In tsA201 cells, α7 subunits assemble by a default pathway since they remain in a single conformation, SH, and assemble into pentamers that are neither functional nor bind Bgt. In SH-SY5Y and PC-12 cells, α7 subunits fold into a second conformation, S-S, and assemble with subunits in the SH conformation into pentamers that function and bind Bgt. The question marks are included in the figure because it is unclear whether the subunits undergo the conformational change before, during, or after assembly into pentamers. If it is assumed that ACh-binding sites can form on S-S subunits at their interface with other subunits, then distinguishable sites can form at interfaces between S-S subunits (open ellipses) and between S-S and SH subunits (filled ellipses).

1997), we found that the ACh-binding sites of $\alpha7/5HT_3$ receptors and the $\alpha7$ receptors from PC12 cells were distinguishable, similar to the ACh-binding sites of muscle AChRs. Muscle AChRs are heteroligomers with two ACh-binding sites that are located at the interface between $\alpha1$ and other subunits. The differences between the two muscle AChR ACh-binding sites are caused by the association of $\alpha1$ subunits with two different subunits, either γ or δ (Blount and Merlie, 1989; Pedersen and Cohen, 1990). As shown in Fig. 7 B, a receptor composed of one subunit in the SH conformation interspersed with four subunits in the S-S conformation could give rise to two different classes of ACh-binding sites. If it is assumed, as with the muscle AChR, that there is one ACh-binding site for each S-S subunit at or near the interface between subunits, ACh-binding sites would exist at two different subunit interfaces. Of the four ACh-binding sites, one would be at the interface between S-S and SH subunits and four at interfaces between two S-S subunits. Generation of two different $\alpha7$ subunit conformations thus creates two different subunit interfaces which, in analogy with the muscle AChR, are needed to form ACh-binding sites with different affinities. By conferring on the receptor the ability to form distinguishable binding sites, different $\alpha7$ subunit conformations would serve the same function as different AChR subunit isoforms. For oligomeric receptors and ion channels, subunit diversity can be generated by transcription of different subunit genes, alternative mRNA splicing, and mRNA editing mechanisms. Our results suggest that protein folding is another mechanism by which differences in subunits are generated.

The authors are grateful to Dr. R. Lukas for the SH-SY5Y cell line stably expressing the rat $\alpha7$ subunit, Dr. J.-L. Eisele for the $\alpha7$ and $\alpha7/5HT_3$ subunit cDNAs, Dr. R. Burry for the PC12 N21 cell line, and to Dr. W.-J. Tang for the mAb 12CA5 hybridoma line. The authors would also like to thank Dr. S. Sisodia and members of the Green laboratory for discussion and comments about this paper.

This work was supported by grants from the National Institutes of Health (W.N. Green and D.S. McGehee), Brain Research Foundation (W.N. Green), and an American Heart Association (Chicago) Senior Fellowship (S. Rakhilin).

Submitted: 20 November 1998
Revised: 1 June 1999
Accepted: 7 June 1999

References

Alkondon, M., and E.X. Albuquerque. 1993. Diversity of nicotinic acetylcholine receptors in rat hippocampal neurons. I. Pharmacological and functional evidence for distinct structural subtypes. *J. Pharmacol. Exp. Ther.* 265:1455–1473.

Alkondon, M., E.S. Rocha, A. Maelicke, and E.X. Albuquerque. 1996. Diversity of nicotinic acetylcholine receptors in rat brain. V. Alpha-bungarotoxin-sensitive nicotinic receptors in olfactory bulb neurons and presynaptic modulation of glutamate release. *J. Pharmacol. Exp. Ther.* 278:1460–1471.

Blount, P., and J.P. Merlie. 1989. Molecular basis of the two nonequivalent ligand binding sites of the muscle nicotinic acetylcholine receptor. *Neuron.* 3:349–357.

Blumenthal, E.M., W.G. Conroy, S.J. Romano, P.D. Kassner, and D.K. Berg. 1997. Detection of functional nicotinic receptors blocked by alpha-bungarotoxin on PC12 cells and dependence of their expression on post-translational events. *J. Neurosci.* 17:6094–6104.

Braakman, I., L.H. Hoover, K.R. Wagner, and A. Helenius. 1991. Folding of influenza hemagglutinin in the endoplasmic reticulum. *J. Cell Biol.* 114:401–411.

Braakman, I., J. Helenius, and A. Helenius. 1992. Manipulating disulfide bond formation and protein folding in the endoplasmic reticulum. *EMBO (Eur. Mol. Biol. Org.) J.* 11:1717–1722.

Breese, C.R., C. Adams, J. Logel, C. Drebing, Y. Rollins, M. Barnhart, B. Sullivan, B.K. Demasters, R. Freedman, and S. Leonard. 1997. Comparison of the regional expression of nicotinic acetylcholine receptor alpha7 mRNA and [125I]-alpha-bungarotoxin binding in human postmortem brain. *J. Comp. Neurol.* 387:385–398.

Broide, R.S., R.T. Robertson, and F.M. Leslie. 1996. Regulation of alpha7 nicotinic acetylcholine receptors in the developing rat somatosensory cortex by thalamocortical afferents. *J. Neurosci.* 16:2956–2971.

Castro, N.G., and E.X. Albuquerque. 1995. Alpha-bungarotoxin-sensitive hippocampal nicotinic receptor channel has a high calcium permeability. *Biophys. J.* 68:516–524.

Chan, J., and M. Quik. 1993. A role for the nicotinic alpha-bungarotoxin receptor in neurite outgrowth in PC12 cells. *Neurosci.* 56:441–451.

Chen, D., and J.W. Patrick. 1997. The alpha-bungarotoxin-binding nicotinic acetylcholine receptor from rat brain contains only the alpha7 subunit. *J. Biol. Chem.* 272:24024–24029.

Chen, D., H. Dang, and J.W. Patrick. 1998. Contributions of N-linked glycosylation to the expression of a functional alpha7-nicotinic receptor in *Xenopus* oocytes. *J. Neurochem.* 70:349–357.

Cheng, S.H., R.J. Gregory, J. Marshall, S. Paul, D.W. Souza, G.A. White, C.R. O'Riordan, and A.E. Smith. 1990. Defective intracellular transport and processing of CFTR is the molecular basis of most cystic fibrosis. *Cell.* 63:827–834.

Clarke, P.B. 1992. The fall and rise of neuronal alpha-bungarotoxin binding proteins. *Trends Pharmacol. Sci.* 13:407–413.

Claudio, T. 1992. Stable expression of heterologous multisubunit protein complexes established by calcium phosphate or lipid mediated cotransfection. *In* Methods in Enzymology: Ion Channels. Vol. 207. 391–408.

Claudio, T., W.N. Green, D.S. Hartman, D. Hayden, H.L. Paulson, F.J. Sigworth, S.M. Sine, and A. Swedlund. 1987. Genetic reconstitution of functional acetylcholine receptor channels in mouse fibroblasts. *Science.* 238: 1688–1694.

Claudio, T., H.L. Paulson, W.N. Green, A.F. Ross, D.S. Hartman, and D.A. Hayden. 1989. Fibroblasts transfected with *Torpedo* acetylcholine receptor β-, γ-, and δ-subunit cDNAs express functional receptors when infected with a retroviral α recombinant. *J. Cell Biol.* 108:2277–2290.

Cooper, S.T., and N.S. Millar. 1997. Host cell-specific folding and assembly of the neuronal nicotinic acetylcholine receptor alpha7 subunit. *J. Neurochem.* 68:2140–2151.

Corringer, P.J., J.L. Galzi, J.L. Eisele, S. Bertrand, J.P. Changeux, and D. Bertrand. 1995. Identification of a new component of the agonist binding site of the nicotinic alpha 7 homooligomeric receptor. *J. Biol. Chem.* 270:11749–11752.

Cortes, D.M., and E. Perozo. 1997. Structural dynamics of the *Streptomyces lividans* K+ channel (SKC1): oligomeric stoichiometry and stability. *Biochemistry.* 36:10343–10352.

Couturier, S., D. Bertrand, J.M. Matter, M.C. Hernandez, S. Bertrand, N. Millar, S. Valera, T. Barkas, and M. Ballivet. 1990. A neuronal nicotinic acetylcholine receptor subunit (alpha 7) is developmentally regulated and forms a homo-oligomeric channel blocked by alpha-BTX. *Neuron.* 5:847–856.

Denning, G.M., M.P. Anderson, J.F. Amara, J. Marshall, A.E. Smith, and M.J. Welsh. 1992. Processing of mutant cystic fibrosis transmembrane conductance regulator is temperature-sensitive. *Nature.* 358:761–764.

Freedman, R., L.E. Adler, P. Bickford, W. Byerley, H. Coon, C.M. Cullum, J.M. Griffith, J.G. Harris, S. Leonard, C. Miller, et al. 1994. Schizophrenia and nicotinic receptors. *Harv. Rev. Psychiatry.* 2:179–192.

Freedman, R., H. Coon, W.M. Myles, U.A. Orr, A. Olincy, A. Davis, M. Polymeropoulos, J. Holik, J. Hopkins, M. Hoff, et al. 1997. Linkage of a neurophysiological deficit in schizophrenia to a chromosome 15 locus. *Proc. Natl. Acad. Sci. USA.* 94:587–592.

Gray, R., A.S. Rajan, K.A. Radcliffe, M. Yakehiro, and J.A. Dani. 1996. Hippocampal synaptic transmission enhanced by low concentrations of nicotine. *Nature.* 383:713–716.

Green, W.N., and N.S. Millar. 1995. Ion-channel assembly. *Trends Neurosci.* 18: 280–287.

Green, W.N., and C.P. Wanamaker. 1997. The role of the cysteine loop in acetylcholine receptor assembly. *J. Biol. Chem.* 272:20945–20953.

Gu, Y., E. Ralston, C. Murphy-Erdosh, and Z.W. Hall. 1989. Acetylcholine receptor in a C2 muscle cell variant is retained in the endoplasmic reticulum. *J. Cell Biol.* 109:729–738.

Hamill, O.P., A. Marty, E. Neher, B. Sakmann, and F.J. Sigworth. 1981. Improved patch-clamp techniques for high-resolution current recordings from cells and cell-free membrane patches. *Pfluegers Arch.* 391:85–100.

Helekar, S.A., and J. Patrick. 1997. Peptidyl prolyl cis-trans isomerase activity of cyclophilin A in functional homo-oligomeric receptor expression. *Proc. Natl. Acad. Sci. USA.* 94:5432–5437.

Helekar, S.A., D. Char, S. Neff, and J. Patrick. 1994. Prolyl isomerase requirement for the expression of functional homo-oligomeric ligand-gated ion channels. *Neuron.* 12:179–189.

Higgins, L.S., and D.K. Berg. 1988. Cyclic AMP-dependent mechanism regulates acetylcholine receptor function on bovine adrenal chromaffin cells and discriminates between new and old receptors. *J Cell Biol.* 107:1157–1165.

Ho, S.N., H.D. Hunt, R.M. Horton, J.K. Pullen, and L.R. Pease. 1989. Site-directed mutagenesis by overlap extension using the polymerase chain reaction. *Gene.* 77:51–59.

Kao, P.N., and A. Karlin. 1986. Acetylcholine receptor binding site contains a disulfide cross-link between adjacent half-cystinyl residues. *J. Biol. Chem.*

261:8085–8088.
Karlin, A., and M.H. Akabas. 1995. Towards a structural basis for the function of nicotinic acetylcholine receptors and their cousins. *Neuron*. 15:1231–1244.
Lindstrom, J.M. 1995. Nicotinic acetylcholine receptors. *In* Handbook of Receptors and Channels. Ligand- and Voltage-gated Ion Channels. R.A. North, editor. CRC Press, Boca Raton, FL. 153–175.
Listerud, M., A.B. Brussaard, P. Devay, D.R. Colman, and L.W. Role. 1991. Functional contribution of neuronal AChR subunits revealed by antisense oligonucleotides. *Science.* 254:1518–1521.
Margiotta, J.F., D.K. Berg, and V.E. Dionne. 1987. Cyclic AMP regulates the proportion of functional acetylcholine receptors on chicken ciliary ganglion neurons. *Proc. Natl. Acad. Sci. USA*. 84:8155–8159.
McGehee, D.S., and L.W. Role. 1995. Physiological diversity of nicotinic acetylcholine receptors expressed by vertebrate neurons. *Annu. Rev. Physiol.* 57: 521–546.
McGehee, D.S., M.J.S. Heath, S. Gelber, P. Devay, and L.W. Role. 1995. Nicotine enhancement of fast excitatory synaptic transmission in CNS by presynaptic receptors. *Science.* 269:1692–1696.
Merlie, J.P., and J. Lindstrom. 1983. Assembly in vivo of mouse muscle acetylcholine receptor: identification of an alpha subunit species that may be an assembly intermediate. *Cell.* 34:747–757.
Mishina, M., T. Tobimatsu, K. Tanaka, Y. Fujita, K. Fukuda, M. Kurasake, H. Takahashi, Y. Morimoto, T. Hirose, S. Inayama, et al. 1985. Location of functional regions of acetylcholine receptor a-subunit by site-directed mutagenesis. *Nature.* 313:364–369.
Pedersen, S.E., and J.B. Cohen. 1990. d-Tubocurarine binding sites are located at alpha-gamma and alpha-delta subunit interfaces of the nicotinic acetylcholine receptor. *Proc. Natl. Acad. Sci. USA*. 87:2785–2789.
Peng, X., M. Katz, V. Gerzanich, R. Anand, and J. Lindstrom. 1994. Human alpha 7 acetylcholine receptor: cloning of the alpha 7 subunit from the SH-SY5Y cell line and determination of pharmacological properties of native receptors and functional alpha 7 homomers expressed in *Xenopus* oocytes. *Mol. Pharmacol.* 45:546–554.
Prusiner, S.B., M.R. Scott, S.J. DeArmound, and F.E. Cohen. 1998. Prion protein biology. *Cell.* 93:337–348.
Puchacz, E., B. Buisson, D. Bertrand, and R.J. Lukas. 1994. Functional expression of nicotinic acetylcholine receptors containing rat alpha 7 subunits in human SH-SY5Y neuroblastoma cells. *FEBS Lett.* 354:155–159.
Pugh, P.C., and D.K. Berg. 1994. Neuronal acetylcholine receptors that bind alpha-bungarotoxin mediate neurite retraction in a calcium-dependent manner. *J. Neurosci.* 14:889–896.
Quik, M., J. Choremis, J. Komourian, R.J. Lukas, and E. Puchacz. 1996. Similarity between rat brain nicotinic alpha-bungarotoxin receptors and stably expressed alpha-bungarotoxin binding sites. *J. Neurochem*. 67:145–154.
Rangwala, F., R.C. Drisdel, S. Rakhilin, E. Ko, P. Atluri, A.B. Harkins, A.P. Fox, S.B. Salman, and W.N. Green. 1997. Neuronal α-bungarotoxin receptors differ structurally from other nicotinic acetylcholine receptors. *J. Neurosci.* 17:8201–8212.
Role, L.W., and D.K. Berg. 1996. Nicotinic receptors in the development and modulation of CNS synapses. *Neuron.* 16:1077–1085.
Ross, A.F., W.N. Green, D.S. Hartman, and T. Claudio. 1991. Efficiency of acetylcholine receptor subunit assembly and its regulation by cAMP. *J. Cell Biol.* 113:623–636.
Sargent, P. 1993. The diversity of neuronal nicotinic acetylcholine receptors. *Annu. Rev. Neurosci.* 16:403–443.
Schoepfer, R., W.G. Conroy, P. Whiting, M. Gore, and J. Lindstrom. 1990. Brain alpha-bungarotoxin binding protein cDNAs and MAbs reveal subtypes of this branch of the ligand-gated ion channel gene superfamily. *Neuron.* 5:35–48.
Seguela, P., J. Wadiche, M.K. Dineley, J.A. Dani, and J.W. Patrick. 1993. Molecular cloning, functional properties, and distribution of rat brain alpha 7: a nicotinic cation channel highly permeable to calcium. *J. Neurosci.* 13:596–604.
Smith, M.M., J. Lindstrom, and J.P. Merlie. 1987. Formation of the α-bungarotoxin binding site and assembly of the acetylcholine receptor subunits occur in the endoplasmic reticulum. *J. Biol. Chem*. 262:4367–4376.
Sumikawa, K., and V.M. Gehle. 1992. Assembly of mutant subunits of the nicotinic acetylcholine receptor lacking the conserved disulfide loop structure. *J. Biol. Chem*. 267:6286–6290.
Swick, A.G., M. Janicot, K.T. Cheneval, J.C. McLenithan, and M.D. Lane. 1992. Promoter-cDNA-directed heterologous protein expression in *Xenopus laevis* oocytes. *Proc. Natl. Acad. Sci. USA*. 89:1812–1816.
Towbin, H., T. Staehelin, and J. Gordon. 1979. Electrophoretic transfer of proteins from polyacrylamide gels to nitrocellulose sheets: procedure and some applications. *Proc. Natl. Acad. Sci. USA*. 76:4350–4354.
Unwin, N. 1993. Neurotransmitter action: opening of ligand-gated ion channels. *Cell.* 72(Suppl.):31–41.
Vijayaraghavan, S., P.C. Pugh, Z.W. Zhang, M.M. Rathouz, and D.K. Berg. 1992. Nicotinic receptors that bind alpha-bungarotoxin on neurons raise intracellular free Ca2+. *Neuron.* 8:353–362.
Wells, G.B., R. Anand, F. Wang, and J. Lindstrom. 1998. Water-soluble nicotinic acetylcholine receptor formed by alpha7 subunit extracellular domains. *J. Biol. Chem*. 273:964–973.
West, A.J., P.J. Bjorkman, D.A. Dougherty, and H.A. Lester. 1997. Expression and circular dichroism studies of the extracellular domain of the alpha subunit of the nicotinic acetylcholine receptor. *J. Biol. Chem*. 272:25468–25473.
Wilson, I.A., H.L. Niman, R.A. Houghten, A.R. Cherenson, M.L. Connolly, and R.A. Lerner. 1984. The structure of an antigenic determinant in a protein. *Cell.* 37:767–778.
Zhang, Z.W., S. Vijayaraghavan, and D.K. Berg. 1994. Neuronal acetylcholine receptors that bind alpha-bungarotoxin with high affinity function as ligand-gated ion channels. *Neuron.* 12:167–177.
Zorumski, C.F., L.L. Thio, K.E. Isenberg, and D.B. Clifford. 1992. Nicotinic acetylcholine currents in cultured postnatal rat hippocampal neurons. *Mol. Pharmacol.* 41:931–936.